



HAL
open science

Use of Ussing Chambers to Measure Paracellular Permeability to Macromolecules in Mouse Intestine

Doriane Aguanno, Bárbara Graziela Postal, Véronique Carrière, Sophie Thenet

► **To cite this version:**

Doriane Aguanno, Bárbara Graziela Postal, Véronique Carrière, Sophie Thenet. Use of Ussing Chambers to Measure Paracellular Permeability to Macromolecules in Mouse Intestine. Kursad Turksen. Permeability Barrier: methods and protocols, 2367, Springer US, pp.1-11, 2021, Methods in Molecular Biology, 978-1-0716-1673-4 (ebook). 10.1007/7651_2021_367 . hal-03971980

HAL Id: hal-03971980

<https://hal.sorbonne-universite.fr/hal-03971980>

Submitted on 1 Mar 2023

HAL is a multi-disciplinary open access archive for the deposit and dissemination of scientific research documents, whether they are published or not. The documents may come from teaching and research institutions in France or abroad, or from public or private research centers.

L'archive ouverte pluridisciplinaire **HAL**, est destinée au dépôt et à la diffusion de documents scientifiques de niveau recherche, publiés ou non, émanant des établissements d'enseignement et de recherche français ou étrangers, des laboratoires publics ou privés.



Distributed under a Creative Commons Attribution - NonCommercial 4.0 International License

Use of Ussing chambers to measure paracellular permeability to macromolecules in mouse intestine

Doriane Aguanno^{1,2}, Barbara Graziela Postal^{1,3,4}, Véronique Carrière^{1,5}, Sophie Thenet^{1,2,5}

¹Centre de Recherche Saint-Antoine, Sorbonne Université, INSERM UMRS 938, Paris, France, ²EPHE, PSL University, Paris, France, ³Université de Paris, Centre de Recherche sur l'Inflammation, INSERM UMR1149, Paris, France, ⁴Biology and Genetics of Bacterial Cell Wall Unit, Pasteur Institute, Paris, France, ⁵ Paris Center for Microbiome Medicine (PaCeMM) FHU, AP-HP, Paris, Ile-de-France, France.

Corresponding author: Sophie Thenet, EPHE, PSL University, Centre de Recherche Saint-Antoine, Sorbonne Université, INSERM UMRS 938, équipe P. Seksik & H. Sokol, 27 rue de Chaligny 75012, Paris, France, email: sophie.thenet@ephe.psl.eu, tel: +33 1 40 01 13 89

Key words: Ussing chambers, intestinal permeability, leak pathway, mouse intestine, FITC-dextran

Running title: Measure of intestinal paracellular permeability using Ussing chambers

Abstract

An increased intestinal permeability has been described in many diseases including inflammatory bowel disease and metabolic disorders, and a better understanding of the contribution of intestinal barrier impairment to pathogenesis is needed. In recent years, attention has been paid to the leak pathway, which is the route of paracellular transport allowing the diffusion of macromolecules through the tight junctions of the intestinal epithelial lining. While the passage of macromolecules by this pathway is very restricted under physiological conditions, its amplification is thought to promote an excessive immune activation in the intestinal mucosa. The Ussing chambers have been widely used to measure both active and passive transepithelial fluxes in intact tissues. In this chapter we present how this simple device can be used to measure paracellular permeability to macromolecules in the mouse intestine. We propose a detailed protocol and describe how to best exploit all the possibilities of this technique, correctly interpret the results and avoid the main pitfalls.

1. Introduction

1 Changes in the properties of the intestinal barrier have been the subject of growing interest in recent years as
2 they have been associated with an increasing number of both digestive and extra-digestive pathologies [1,2]. In
3 addition, the explosion of research on the intestinal microbiota has raised more and more questions requiring a
4 better understanding of the reciprocal interactions between the microorganisms that are residing in the intestinal
5 lumen and the host. At the center of these interactions, the intestinal barrier is a complex entity comprising the
6 mucus layer covering the epithelium, antimicrobial peptides and the underlying immune system, which
7 cooperate together to protect the host against unwanted intrusion of harmful molecules or microorganisms and to
8 prevent excessive immune activation. The epithelial cell monolayer and the intercellular junctions that tightly
9 connect epithelial cells constitute the most crucial determinants of the physical barrier, acting as the gate-keeper
10 between the external environment (i.e. the lumen content) and the remainder of the body. Tight junctions (TJ)
11 form a selectively permeable barrier and constitute the rate-limiting step of paracellular transport, i.e. the passive
12 flux of solutes through the space between cells. Tight junctions are made of highly dynamic and regulated
13 molecular complexes forming an apical belt connected to the cell cytoskeleton [3,4]. The intestinal epithelium is
14 physiologically more permeable than other barriers in the body (such as the skin, the bladder, the distal segments
15 of the renal tubules, the blood-brain barrier, etc...), making paracellular permeability through TJ an important
16 contributor of transepithelial flux in this epithelium. A very fine control of paracellular permeability, decreasing
17 from the small intestine to the colon and along the crypto-villous axis in the small intestine, is essential to
18 maintain the function and homeostasis of the intestinal mucosa [4]. An intestinal hyperpermeability has been
19 described in many pathological conditions [2] and the current paradigm proposes that the increased or
20 uncontrolled passage of dietary or bacterial-derived molecules from the intestinal lumen can initiate (or at least
21 contribute to) the inflammation observed in these pathologies, both in acute inflammatory states as in
22 inflammatory bowel disease [2] as well as in the low-grade inflammation observed in metabolic diseases [5].
23 To better understand how gut barrier disruption can contribute to pathogenesis, there is a need to accurately
24 measure variations of intestinal permeability in human samples and in animal experimental models. The Ussing
25 chamber is a system that allows precise measurement of solutes flow through intact tissues. Initially designed by
26 the Danish Biologist Hans Ussing to measure active ionic fluxes in frog skin [6,7]. Ussing chambers turned out
27 to be also an accurate tool for assessing the passive flux of macromolecules between cells (i.e. paracellular
28 permeability) in many epithelia, both with respect to ions and to macromolecules, whose control is ensured by
29 distinct mechanisms [8] (see also chapter "Rapid evaluation of intestinal paracellular permeability using the
30
31
32
33
34
35
36
37
38
39
40
41
42
43
44
45
46
47
48
49
50
51
52
53
54
55
56
57
58
59
60
61
62
63
64
65

human enterocytic-like Caco-2/TC7 cell line" by Postal et al. in this book). The measurement of ion permeability (ionic conductance) by measurement of transepithelial resistance (TEER) in Ussing chambers has been the subject of numerous reviews [6,9,10] and will not be discussed here. This chapter will focus on the use of Ussing chambers for the measurement of the permeability to macromolecules, which are probably more specifically involved in the initiation of local inflammatory response at the level of the intestinal mucosa and, ultimately, in other tissues, leading to systemic inflammation.

The design of the Ussing chamber is illustrated in Figure 1: the intestinal tissue sample is mounted at the interface of two hemi-chambers bathed with an oxygenated physiological buffer such as Ringer solution and maintained at 37°C. The mucosal (also referred to as the apical or luminal) side of the tissue is facing one chamber half, whereas the serosal (also referred to as the basolateral) side is facing the other half-chamber. After a short period of equilibration, a known quantity of fluorescent tracer is added in the luminal chamber and its passage into the serosal chamber through the tissue is measured over time. The system is remarkably simple and it can be coupled with measure of the TEER [10]. Measuring paracellular permeability in mouse gut with Ussing chambers offers access to information that cannot be provided by overall permeability measurements such as the force-feeding of a tracer and its measurement in blood, another commonly used method to assess gut permeability [11]. The first one is that the permeability of distinct segments of the intestine can be measured specifically. Several genetic modifications give rise to a moderate hyperpermeability in all intestinal segments [12,11] but in other experimental conditions, the permeability has been described to be differentially modulated along the digestive tract: for example, whereas the permeability was similarly increased in jejunum and ileum in mice fed a high fat diet, the hyperpermeability was much more marked in the jejunum than in the ileum in Ob/Ob mice [13]. A time-course study conducted in rats fed a high fat diet revealed that changes in paracellular permeability (assessed by flux of FITC-dextran 4 kDa) and transcellular permeability (assessed by flux of horseradish peroxidase) in the jejunum, ileum, cecum and colon changed during the first weeks of the diet in a region-dependent manner [14].

A second asset of Ussing chamber is that permeability to tracers of different sizes can be assessed on the same sample. The importance of taking into account the permeability to macromolecules can be illustrated by the history of scientific work on occludin, a TJ-associated MARVEL protein (TAMP): measurement of ionic conductance and mannitol flux in the colon of occludin knockout mice showed no difference compared to wild type mice and had temporarily led to the conclusion that occludin had no essential role in the barrier function [15]. A few years later, studies on cultured cell models using a variety of tracers ranging from mannitol to 70

1 kDa dextran demonstrated that occludin is in fact crucial for controlling permeability to macromolecules [16,17],
2 as does tricellulin, another TAMP protein, which is mainly localized at tricellular junctions [18,3]. It has now
3 become clear that the permeability to ions and to small molecules is controlled by proteins that differ in part
4 from those involved in the control of the permeability to macromolecules [8,3], with both common and distinct
5 regulatory mechanisms. Much remains to be discovered in this area and thus, the variations in epithelial
6 permeability under different pathophysiological conditions must consider potential impairment of the different
7 paracellular routes.
8
9
10
11
12
13

14 **2. Materials**

- 15 - Acrylic Ussing chambers placed on a heating block (EM-PMBLTY-6, World Precision Instruments, Figure 1).
16
17 The system must be connected to a circulating water bath.
18
19 - Tissue sliders with a 2mm ϕ aperture and matching the Ussing chambers (P2407, World Precision Instruments).
20
21 See Note 1 and Figure 1.
22
23 - Plugs for closing electrodes holes (P2023, World Precision Instruments)
24
25 - Oxygenation equipment: 95% O₂ + 5% CO₂ (carbogen) gas bottle, compatible manometer and control valve
26 system (See Note 2).
27
28 - Ringer buffer solution (115mM NaCl, 25mM NaHCO₃, 1.2mM MgCl₂, 1.2mM CaCl₂, 2.4mM K₂HPO₄,
29 0.4mM KH₂PO₄) maintained at 37°C (See Note 3)
30
31 - Phosphate Buffer Saline (PBS) solution containing 1 mM CaCl₂ and 0.5 mM MgCl₂
32
33 - 40 mg/mL stock solution of FITC-labeled dextran 4 kD, FD4. See Note 4.
34
35 - FITC-labeled dextran 4 kD standard concentrations (ranging from 10 μ g/mL to 0.01 μ g/mL)
36
37 - Petri dishes
38
39 - Syringes and pipette tips for flushing
40
41 - Surgical vascular ball-tip and straight scissors, forceps
42
43 - 96 well-plate and microplate fluorometer
44
45
46
47
48
49
50
51

52 **3. Protocols**

53 **3.1. Setup of Ussing chambers**

- 54 1. Prior to the experiment, configure the circulating water bath on 42°C to maintain chambers at
55 37°C throughout the experiment and maintain Ringer solution and FD4 solution at 37°C.
56
57
58
59
60
61
62
63
64
65

2. Prepare the setup by placing the paired acrylic chambers onto the heating block (Figure 1A and B). If no electrodes are used (for TEER measurements), the holes must be sealed by using appropriate tips.

3.2. Murine tissue dissection and mounting

1. After euthanasia, perform a midline incision to dissect the appropriate segment(s) to be analyzed, the small intestine and/or the colon. Depending on the numbers of replicates needed, the length of the sample will vary. A margin of half a centimeter should be added to flush the intestinal lumen without harming the mucosa (See Notes 5, 6 and 7).
2. Using a syringe mounted a pipette tip, gently flush with cold PBS solution the intestinal lumen to remove feces, which can be collected.
3. In a petri dish, cut the sample into 1cm-long segments. Each segment will be mounted in a separate slider (Figure 1B and C).
4. Using surgical vascular ball-tip scissors, open the segment of intestinal tube by performing a longitudinal incision, leaving the mucosal surface facing up (Figure 1C).
5. With forceps, transfer the sample onto the tissue slider keeping the mucosa facing up (Figure 1C).
6. Seal the slider, and place it on a paper soaked with PBS while waiting to be placed within the system.
7. Insert the slider with the mounted tissue between Ussing chambers and seal the system by firmly screwing each chamber. Take care to place the mucosal sides of all samples the same side (for example, the transparent part of the slider can be used as a visual clue for mucosal side).
8. Gently add 2mL of Ringer solution per chamber and connect to the oxygenation system.
9. Leave each sample for equilibration at least 25 min (the duration of this equilibration phase will depend on the number of chambers to be mounted but should not exceed one hour). Repeat to mount all chambers. On an indicative basis, to dissect and mount two replicates of tissue on two different sliders, 5 min are required and thus 30 min in total for 12 chambers.

3.3. FITC-labeled dextran 4 kDa (FD4) addition and flux measurements

1. After equilibration, take and discard 100 μ L of media from the mucosal chamber. Add 100 μ L of FD4 stock solution (40mg/mL) to reach a final concentration of 2mg/mL. Additional drugs

1
2 or molecules of interest can be added to either the mucosal chamber or the serosal chamber at
3 this stage or later (See Note 8 and Figure 2).

- 4
5
6
7
8
9
10
11
12
13
14
15
16
17
18
19
20
21
22
23
24
25
2. Take 150 μ L from each serosal chamber. These samples represent the basal fluorescence level at time-point 0.
 3. Immediately read the fluorescence levels in 96-well plate using a fluorometer and standard concentrations to determine the tracer concentration in serosal samples.
 4. Put the 150 μ L samples back into each corresponding chamber to maintain unchanged media volume throughout the experiment.
 5. Repeat steps 2, 3 and 4 every 15min (at least for 45min) to measure the FD4 flux over time (See Note 9).
 6. Mucosal media can be sampled at the end of the experiment to measure lactate dehydrogenase release, which is proportional to cell lysis, to assess tissue viability [19].

26 **3.4. Disassembly and cleaning of the system**

- 27
28
29
30
31
32
33
34
35
36
37
38
39
40
41
42
43
44
45
46
47
1. Turn off the oxygenation system, oxygenation valves and the heating system.
 2. Remove Ussing chambers from the heating block, empty the remaining media and soak them for half an hour in antibacterial detergent cleaning solution.
 3. Remove the remaining tissues from the sliders and gently brush them with a toothbrush. Soak them for half an hour in antibacterial detergent cleaning solution.
 4. Thoroughly rinse 3 times the chambers and slides in clean water (using filtered water for the last rinse) and leave them to dry.
 5. Carefully flush the media reservoir and gas channels with air using a syringe to remove remaining water droplets.

48 **3.5. Data analysis**

- 49
50
51
52
53
54
55
56
57
58
59
60
61
62
63
64
65
1. Once all the concentrations of the fluorescent tracer are determined in each sample for the whole time-course, data can be analyzed as FD4 passage over time. Choose an appropriate part of the curve allowing to apply a linear regression (see Note 10) and calculate the slope of FD4 passage for each sample. This value is the final output parameter used to pool samples per condition and to compare conditions.

- 1
2
3
4
5
6
2. The above kinetics approach allows to identify damaged tissues through unexpected high values of fluorescence or slope changes. Other analyses methods are possible (see Note 10).

4. Notes

- 7
8
9
10
11
12
13
14
15
16
17
18
19
20
21
22
23
24
25
26
27
28
29
30
31
32
33
34
35
36
37
38
39
40
41
42
43
44
45
46
47
48
49
50
51
52
53
54
55
56
57
58
59
60
61
62
63
64
65
1. Depending on the available equipment and tissue samples, different types of tissue sliders with varying aperture diameters can be used. For mouse intestine, 2mm \varnothing aperture sliders are well suited (1cm tissue samples). Five-mm \varnothing aperture sliders with mounting pins allow a larger window of passage but this requires having larger tissue samples (1.5 cm), for example human surgical specimen. Smaller aperture sliders (0.8mm \varnothing) are adapted for small tissues such as biopsies.
 2. The manometer must include a specific valve allowing a fine control of the gas pressure in order to maintain it low enough to generate a gentle bubbling in Ussing chambers.
 3. Tissues can be also kept and processed for measurements in Ussing chambers in culture media such as Dulbecco's Modified Eagle Medium (DMEM). Pay attention to glucose concentration, as it has been shown that a high glucose concentration leads to an opening of intercellular junctions and increase in paracellular permeability [7]. In any case, media should be phenol red-free to avoid noise autofluorescence.
 4. The intestinal permeability can be assessed by the passage of different fluorescent dextrans with various sizes ranging from 4kDa to 150kDa, or smaller molecules such as FITC-labeled sulfonic acid 0.4kDa [20]. The maximum size of a molecule so that it can cross the epithelium by the paracellular route remains debated. Its diameter could reach 100 Å (10 nm) [17,3], which corresponds to the diameter of the "tube" formed at a tricellular junction [21]. It should be noted that many authors still consider that flux of tracers larger than 40 kDa evaluate exclusively the transcellular pathway; it is likely that, depending on the conditions, a mix of paracellular and transcellular pathways is assessed using such large tracers. It must also be kept in mind that epithelial damages generate an unrestricted, TJ-independent pathway [4]. In addition, fluorescent bacteria can be used to assess their passage across the intestinal barrier [12,22]. Dextrans labeled with other fluorochromes such as TRITC-dextrans can also be used. The wavelengths of excitation and emission will depend on the fluorochrome and must be compatible with your microplate fluorometer. For FITC-Dextran, read the fluorescence with the following wavelengths parameters: 485nm for excitation and 535nm for emission.

- 1
2
3
4
5
6
7
8
9
10
11
12
13
14
15
16
17
18
19
20
21
22
23
24
25
26
27
28
29
30
31
32
33
34
35
36
37
38
39
40
41
42
43
44
45
46
47
48
49
50
51
52
53
54
55
56
57
58
59
60
61
62
63
64
65
5. For studies on mouse tissues, the seromuscular layer can be gently dissected and stripped from the mucosal layer [6], but this procedure could damage the tissue integrity and is not obligatory, as it has been shown in several studies [12,22,11]. To our knowledge, dissection of the submucosa and muscle plane is mandatorily performed for studies on human intestinal samples.
6. One can choose to compare intestinal permeability between the different gut segments (small intestine versus colon which feature distinct barrier function properties), or to analyze a single segment or even specific anatomical parts such as Peyer's patches [12]. It is worth noting that the chosen segment of the digestive track will determine the number of possible replicates per mouse, the colon being much shorter than the jejunum for example.
7. Depending on the work hypothesis, the design of the experiment should consider the number of available Ussing chambers (6, 12, etc), the different experimental conditions and the number of samples that can be dissected from a single intestinal segment. If possible, two replicates per mouse and segment for a single condition should be analyzed for a more reliable analysis (Figure 2C). As an example, with 12 available Ussing chambers and in the case of 3 experimental conditions, 2 mice per condition can be analyzed in a single run by mounting duplicate colon samples for each mouse. Thus, to analyze 8 animals from a same condition, four runs will be needed.
8. One of the advantages of Ussing chambers is the possibility to add treatments directly on the tissue *ex vivo* in a polarized manner (Figure 2A-C). Compounds can be added either in the mucosal or serosal chamber. If added compounds lead to an increase in the tracer passage, the analysis should be performed on the linear section of the permeability curve (Figure 2A-C). If the effect of the *ex vivo* treatment is observed within a timeframe compatible with the maintenance of the tissue viability, the two slopes of the tracer flow, before and after treatment, can be determined [20].
9. If the tissues are kept in the system too long and their viability decline, the fluorescent tracer concentration will reach unusually high values. It is thus important to determine the optimal duration of the experiment in the course of optimization on test samples. As an example, in our conditions, the FD4 flux was still linear at 105 minutes (Figure 2A). In the case of human biopsies or samples, the post-surgery delay is variable and must be taken into account. Keeping the sample into DMEM rather than a saline solution can help to preserve its viability [20]. If the human or mouse tissues have been impaired during dissection or mounting, aberrant values of fluorescence will be rapidly detected.

10. In a kinetic approach, FD4 detected in the serosal chamber can be plotted over time as either absolute values (quantity of tracer) or as percentage of the initial tracer quantity injected in the mucosal chamber [20]. The section of the curve of FD4 flux chosen to carry a linear regression analysis to obtain slope values should be the same for all replicates from a single experiment. Alternatively, the FD4 concentration measured at the end of the experiment can be expressed as flux (quantity/time/area (depending of aperture surface of the sliders)) [12,23,11]. However, the slope values of the tracer passage measured over time seem to be more consistent between replicates than single time-point values.

Acknowledgments

This work was supported by the Association François Aupetit (AFA) ; Institut National de la Santé et de la Recherche Médicale; Sorbonne Université; Ecole Pratique des Hautes Etudes ; the Brazilian government's Science Without Borders Program. DA was the recipient of a fellowship from CORDDIM Ile de France. B.G.P. received a doctoral fellowship (CNPq 207303/2014-2).

References:

1. Konig, J., Wells, J., Cani, P.D., Garcia-Rodenas, C.L., MacDonald, T., Mercenier, A., Whyte, J., Troost, F., Brummer, R.J.: Human Intestinal Barrier Function in Health and Disease. *Clinical and translational gastroenterology* **7**(10), e196 (2016). doi:10.1038/ctg.2016.54
2. Odenwald, M.A., Turner, J.R.: The intestinal epithelial barrier: a therapeutic target? *Nat Rev Gastroenterol Hepatol* **14**(1), 9-21 (2017). doi:10.1038/nrgastro.2016.169
3. Krug, S.M., Schulzke, J.D., Fromm, M.: Tight junction, selective permeability, and related diseases. *Semin Cell Dev Biol* **36**, 166-176 (2014). doi:10.1016/j.semcdb.2014.09.002
4. Buckley, A., Turner, J.R.: Cell Biology of Tight Junction Barrier Regulation and Mucosal Disease. *Cold Spring Harb Perspect Biol* **10**(1) (2018). doi:10.1101/cshperspect.a029314
5. Tilg, H., Zmora, N., Adolph, T.E., Elinav, E.: The intestinal microbiota fuelling metabolic inflammation. *Nature reviews. Immunology* **20**(1), 40-54 (2020). doi:10.1038/s41577-019-0198-4
6. Clarke, L.L.: A guide to Ussing chamber studies of mouse intestine. *Am J Physiol Gastrointest Liver Physiol* **296**(6), G1151-1166 (2009). doi:10.1152/ajpgi.90649.2008
7. Herrmann, J.R., Turner, J.R.: Beyond Ussing's chambers: contemporary thoughts on integration of transepithelial transport. *Am J Physiol Cell Physiol* **310**(6), C423-431 (2016). doi:10.1152/ajpcell.00348.2015
8. Shen, L., Weber, C.R., Raleigh, D.R., Yu, D., Turner, J.R.: Tight junction pore and leak pathways: a dynamic duo. *Annu Rev Physiol* **73**, 283-309 (2011). doi:10.1146/annurev-physiol-012110-142150
9. Westerhout, J., Wortelboer, H., Verhoeckx, K.: Ussing Chamber. In: Verhoeckx, K., Cotter, P., Lopez-Exposito, I., Kleiveland, C., Lea, T., Mackie, A., Requena, T., Swiatecka, D., Wichers, H. (eds.) *The Impact of Food Bioactives on Health: in vitro and ex vivo models*. pp. 263-273. Cham (CH) (2015)
10. Thomson, A., Smart, K., Somerville, M.S., Lauder, S.N., Appanna, G., Horwood, J., Sunder Raj, L., Srivastava, B., Durai, D., Scurr, M.J., Keita, A.V., Gallimore, A.M., Godkin, A.: The Ussing chamber system for measuring intestinal permeability in health and disease. *BMC Gastroenterol* **19**(1), 98 (2019). doi:10.1186/s12876-019-1002-4

11. Petit, C.S., Barreau, F., Besnier, L., Gandille, P., Riveau, B., Chateau, D., Roy, M., Berrebi, D., Svrcek, M., Cardot, P., Rousset, M., Clair, C., Thenet, S.: Requirement of cellular prion protein for intestinal barrier function and mislocalization in patients with inflammatory bowel disease. *Gastroenterology* **143**(1), 122-132 e115 (2012). doi:10.1053/j.gastro.2012.03.029
12. Barreau, F., Meinzer, U., Chareyre, F., Berrebi, D., Niwa-Kawakita, M., Dussaillant, M., Foligne, B., Ollendorff, V., Heyman, M., Bonacorsi, S., Lesuffleur, T., Sterkers, G., Giovannini, M., Hugot, J.P.: CARD15/NOD2 is required for Peyer's patches homeostasis in mice. *PLoS One* **2**(6), e523 (2007). doi:10.1371/journal.pone.0000523
13. Johnson, A.M., Costanzo, A., Gareau, M.G., Armando, A.M., Quehenberger, O., Jameson, J.M., Olefsky, J.M.: High fat diet causes depletion of intestinal eosinophils associated with intestinal permeability. *PLoS One* **10**(4), e0122195 (2015). doi:10.1371/journal.pone.0122195
14. Hamilton, M.K., Boudry, G., Lemay, D.G., Raybould, H.E.: Changes in intestinal barrier function and gut microbiota in high-fat diet-fed rats are dynamic and region dependent. *Am J Physiol Gastrointest Liver Physiol* **308**(10), G840-851 (2015). doi:10.1152/ajpgi.00029.2015
15. Schulzke, J.D., Gitter, A.H., Mankertz, J., Spiegel, S., Seidler, U., Amasheh, S., Saitou, M., Tsukita, S., Fromm, M.: Epithelial transport and barrier function in occludin-deficient mice. *Biochim Biophys Acta* **1669**(1), 34-42 (2005). doi:10.1016/j.bbamem.2005.01.008
16. Al-Sadi, R., Khatib, K., Guo, S., Ye, D., Youssef, M., Ma, T.: Occludin regulates macromolecule flux across the intestinal epithelial tight junction barrier. *Am J Physiol Gastrointest Liver Physiol* **300**(6), G1054-1064 (2011). doi:10.1152/ajpgi.00055.2011
17. Buschmann, M.M., Shen, L., Rajapakse, H., Raleigh, D.R., Wang, Y., Wang, Y., Lingaraju, A., Zha, J., Abbott, E., McAuley, E.M., Breskin, L.A., Wu, L., Anderson, K., Turner, J.R., Weber, C.R.: Occludin OCEL-domain interactions are required for maintenance and regulation of the tight junction barrier to macromolecular flux. *Mol Biol Cell* **24**(19), 3056-3068 (2013). doi:10.1091/mbc.E12-09-0688
18. Krug, S.M., Amasheh, S., Richter, J.F., Milatz, S., Gunzel, D., Westphal, J.K., Huber, O., Schulzke, J.D., Fromm, M.: Tricellulin forms a barrier to macromolecules in tricellular tight junctions without affecting ion permeability. *Mol Biol Cell* **20**(16), 3713-3724 (2009). doi:10.1091/mbc.E09-01-0080
19. Soderholm, J.D., Hedman, L., Artursson, P., Franzen, L., Larsson, J., Pantzar, N., Permert, J., Olaison, G.: Integrity and metabolism of human ileal mucosa in vitro in the Ussing chamber. *Acta Physiol Scand* **162**(1), 47-56 (1998). doi:10.1046/j.1365-201X.1998.0248f.x
20. Genser, L., Aguanno, D., Soula, H.A., Dong, L., Trystram, L., Assmann, K., Salem, J.E., Vaillant, J.C., Oppert, J.M., Laugerette, F., Michalski, M.C., Wind, P., Rousset, M., Brot-Laroche, E., Leturque, A., Clement, K., Thenet, S., Poitou, C.: Increased jejunal permeability in human obesity is revealed by a lipid challenge and is linked to inflammation and type 2 diabetes. *J Pathol* **246**(2), 217-230 (2018). doi:10.1002/path.5134
21. Furuse, M., Izumi, Y., Oda, Y., Higashi, T., Iwamoto, N.: Molecular organization of tricellular tight junctions. *Tissue Barriers* **2**, e28960 (2014). doi:10.4161/tisb.28960
22. Barreau, F., Madre, C., Meinzer, U., Berrebi, D., Dussaillant, M., Merlin, F., Eckmann, L., Karin, M., Sterkers, G., Bonacorsi, S., Lesuffleur, T., Hugot, J.P.: Nod2 regulates the host response towards microflora by modulating T cell function and epithelial permeability in mouse Peyer's patches. *Gut* **59**(2), 207-217 (2010). doi:10.1136/gut.2008.171546
23. Laukoetter, M.G., Nava, P., Lee, W.Y., Severson, E.A., Capaldo, C.T., Babbitt, B.A., Williams, I.R., Koval, M., Peatman, E., Campbell, J.A., Dermody, T.S., Nusrat, A., Parkos, C.A.: JAM-A regulates permeability and inflammation in the intestine in vivo. *J Exp Med* **204**(13), 3067-3076 (2007). doi:10.1084/jem.20071416

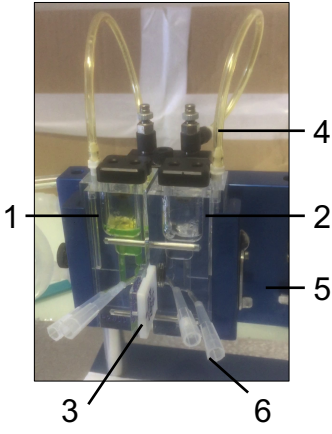
1
2 **Figure Legends**

3
4 **Figure 1: Ussing chambers system.** A) Photograph of a mounted and operating Ussing chamber system. 1:
5 Mucosal (apical) Ussing chamber containing FITC-dextran 4kDa; 2: Serosal (basolateral) Ussing chamber; 3:
6 Tissue slider mounted with a sample; 4: oxygenation tube; 5: heating block; 6: plugs closing electrodes gaps. B)
7 Photographs of paired Ussing chambers (top) and tissue sliders (bottom). 7: moieties of 2mm \varnothing aperture tissue
8 sliders; 8: moieties of 5mm \varnothing aperture tissue sliders with mounting pins. C) Schematic representation of intestinal
9 segment dissection and mounting onto tissue sliders. The intestinal tube (approximately 1cm long segment) is
10 opened by performing a longitudinal incision, leaving the mucosal surface facing up. The inner mucosal surface
11 (luminal layer) corresponds to the apical side of the epithelium while the outward surface corresponds to the serosal
12 side (basolateral compartment). The sample is gently transferred (mucosal side facing up) onto the tissue slider
13 (the opaque one represented in gray) and centered on the aperture. The second moiety of the tissue slider (the
14 transparent one represented in white) is then placed on top to block the sample. Both sliders are then placed
15 between paired Ussing chambers. The chamber facing the mucosa corresponds to the luminal or apical pole of the
16 epithelium while the chamber facing the serosal layer corresponds to the basolateral side (inner body compartment).
17
18
19
20
21
22
23
24
25
26
27
28
29
30
31

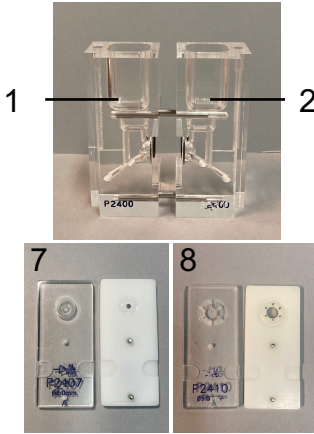
32 **Figure 2: Example of permeability to FITC-Dextran 4kDa (FD4) measured in mouse ileum with Ussing**
33 **chambers.** A) FD4 passage measured over time in control or EGTA-treated ileum samples. EGTA is a calcium
34 chelator known to rapidly disrupt intercellular junctions and thus leading to an increased paracellular permeability.
35 EGTA was added in the mucosal chamber together with FD4 stock solution. Data are presented as the percentage
36 of tracer in the serosal chamber over time. For each condition (control, EGTA 5mM, EGTA 15mM), two replicates
37 of ileum samples were monitored (6 chambers). B) Linear regression of the corresponding FD4 flux curves. The
38 linear regression was applied on a linear part of FD4 kinetics. The first time points were not included to take into
39 account EGTA treatment effects. The obtained slope values for each curve were then analyzed as the output FD4
40 permeability parameter. C) EGTA treatment effects on FD4 permeability in ileum. The experiment described in
41 A was performed with two mice (12 chambers for a single run). Individual slope values of FD4 flux are presented
42 in C for each condition (control, EGTA 5mM, EGTA 15mM) for two mice (represented by square and circle
43 symbols) in duplicate. When further analyzing data, the replicates of each mouse are averaged.
44
45
46
47
48
49
50
51
52
53
54
55
56
57
58
59
60
61
62
63
64
65

Figure 1

A



B



C

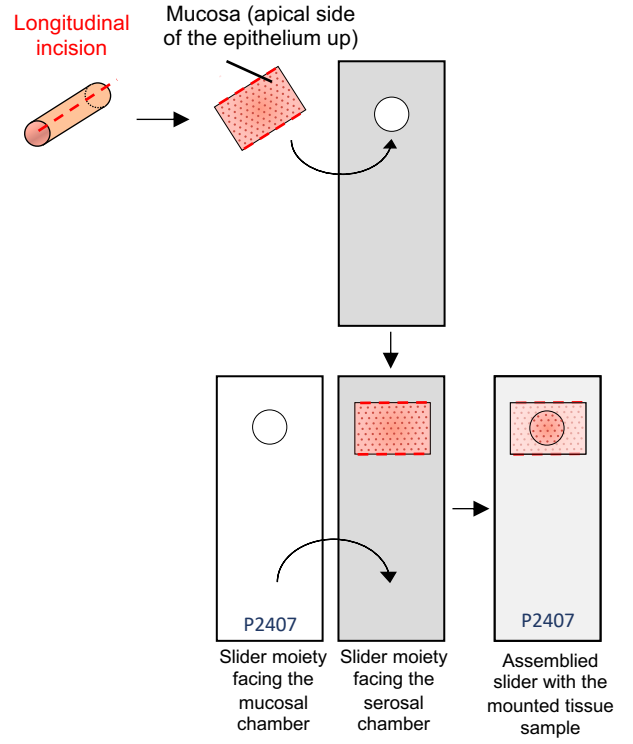
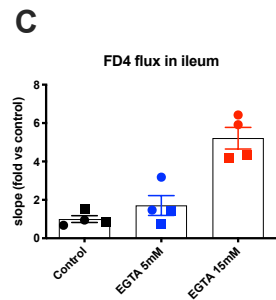
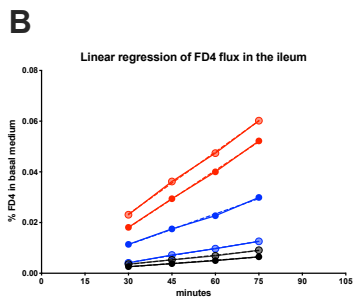
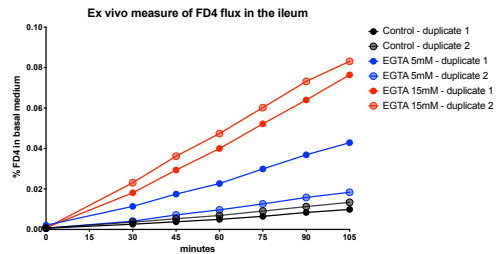


Figure 1

Figure 2**Figure 2**